Available online at BCREC website: https://bcrec.id

Bulletin of Chemical Reaction Engineering & Catalysis, 18 (2) 2023, 331-343

Research Article

Synthesis of NiO/Ni Electrocatalyst at Different pH Values and the Application for Electrochemical Degradation of Textile Waste

Ni Made Wiratini*

Department of Chemistry, Universitas Pendidikan Ganesha, Singaraja, Indonesia.

Received: 21st June 2023; Revised: 29th July 2023; Accepted: 30th July 2023
Available online: 2nd August 2023; Published regularly: August 2023

Abstract

An electrocatalyst is a material that exhibits catalytic activity for electrochemical reactions. The electrocatalytic properties within electrochemical cells can be enhanced by modifying the electrode through an electrodeposition process. Therefore, this study aimed to synthesize NiO/Ni electrocatalyst using the electrodeposition method at pH values of 8, 10, and 12. The NiO/Ni generated was applied in the electrochemical degradation of textile waste under specific operating conditions, including pH = 4, NaCl concentration of 0.05 M, DC voltage of 9 volts, and varying degradation times of 60, 120, 180, and 240 min. Based on the results, the XRD diffractograms revealed the presence of NiO peaks at 2θ = 43.5°, 63.1°, and 75.4°, and Ni peaks at 2θ = 51.9°. SEM-EDX analysis showed that NiO/Ni was deposited on the graphite surface in the form of spheres and granules. FTIR indicated the presence of Ni–O bonds at 501 cm^{-1}, and GSA demonstrated that NiO/Ni exhibited mesoporous properties. The NiO/Ni at pH = 10 had the highest surface area, pore volume, and current response compared to graphite, as well as the electrocatalyst produced at pH of 8 and 12. Additionally, the electrochemical degradation of textile waste using NiO/Ni at pH = 10 led to the highest reduction in absorbance efficiency, chemical oxygen demand (COD), and ammonia, with respective values of 96.80, 96.15, and 87.34%.

Keywords: NiO/Ni electrocatalyst; electrochemical degradation; textile waste

How to Cite: N.M. Wiratini (2023). Synthesis of NiO/Ni Electrocatalyst at Different pH Values and the Application for Electrochemical Degradation of Textile Waste. *Bulletin of Chemical Reaction Engineering & Catalysis*, 18(2), 331-343 (doi: 10.9767/bcrec.18958)

Permalink/DOI: https://doi.org/10.9767/bcrec.18958

1. Introduction

Electrocatalyst is material that facilitates electrochemical reactions and plays a crucial role in various study fields, including wastewater treatment [1]. Extensive investigations have been conducted to develop electrocatalyst for reduction and oxidation processes, based on both precious metals, such as platinum (Pt) and aurum (Au), as well as non-platinum metals encompassing single, binary, ternary, or other alloys. Whilst Pt exhibits superior performance, its high price necessitates the exploration of alternative electrocatalyst with comparable efficiency and lower production costs [2]. Among these alternatives, metal oxides have garnered significant attention due to the unique physicochemical properties possessed, leading to their attractiveness for diverse fields including electrochemistry, catalysis, corrosion, spintronics, and optoelectronics [3].

Several metal oxides, such as IrO_2 and SnO_2, have been used as electrocatalyst for Ti electrodes in the electrooxidation of phenols. The results showed that Ti/IrO_2 and Ti/SnO_2 achieved degradation efficiencies of 71% and 90%, respec-

* Corresponding Author.
Email: made.wiratini@undiksha.ac.id (N.M. Wiratini)

tively. These active oxides function as effective electrocatalyst with excellent catalytic activity and durability [1]. Furthermore, the combination of a graphite electrode with iron silica mesoporous electrocatalyst employed in the electro-fenton degradation of rhodamine B yielded a 97.7% reduction in the color of rhodamine B and 35.1% total organic carbon (TOC). Similar results were observed when applied to textile waste, with a 97% reduction in color and 39% TOC [3].

Nickel (Ni) is used as an electrocatalyst for both anodic and cathodic reactions [4], offering numerous advantages over other catalysts, such as high overpotential, stability, electrical conductivity, catalytic activity, and resistance to CO gas poisoning [5]. When zeolite is impregnated with this metal, Ni exhibits high activity and stability even under varying temperatures [6]. The activity of Ni can be enhanced through various strategies including coating with Mn [7], combination with iron [8], and precipitation with SiO_2 [9]. Notably, in urea electrooxidation, Ni-P mesopore nano catalysts show superior activity and stability compared to Ni nanocatalysts [5]. Furthermore, Ni-Zn electrocatalyst exhibits excellent electrocatalytic performance, large surface area, and high electrical conductivity in hydrazine electrooxidation [10]. Bimetallic hydroxide catalysts composed of nickel and cobalt, synthesized through electrodeposition, exhibit the ability to inhibit water electrolysis reactions and enhance the efficiency of urea electrolysis. They have significant potential for applications in wastewater remediation, hydrogen production, electrochemical sensors, and fuel cells [11]. NiO, a metal oxide with substantial catalyst potential, is widely employed as an electrode material, specifically as an anode [12,13]. Additionally, it has been successfully synthesized in various forms, such as NiO/fluorine-doped tin oxide coated glass substrates (NiO/FTO/Glass) [14] and mesoporous NiO (OM−NiO) nanosheets [5].

Electrocatalyst from metals and metal oxides can be prepared using several methods, including thermal decomposition, solvent impregnation, spray pyrolysis, hydrothermal, and electrodeposition, each with different advantages and disadvantages. In general, some weaknesses arise in terms of cost, product homogeneity, and the strength of the bond between the supporting material and the metal oxide. However, the electrodeposition method offers various advantages, such as large deposition surface area, more homogeneous particle distribution, easy and automatic implementation, low cost, and fast deposition rate [15]. For instance, electrochemical studies revealed Cu-doped NiO (NiO:Cu) thin films synthesized by electrodeposition to be good candidates for magnetic applications [16].

The velocity of electrodeposition is affected by the migration force, which is proportional to the applied potential. This deposition speed significantly impacts the morphology and quantity of the produced metal oxide [17]. The properties of metal oxides strongly influence their activity. Furthermore, the presence of a porous structure and a large surface area enhances their catalytic activity [18]. The electrodeposition of NiO/Ni is more thermodynamically favorable under high pH (alkaline) conditions. Pourbaix diagrams provide a comprehensive illustration of the relationship between potential and pH, indicating that NiO/Ni formation occurs under alkaline pH electrodeposition conditions [13,19,20]. The pH parameter during the electrodeposition process greatly influences the structure, morphology, and electrochemical properties of the synthesized NiO/Ni. Electrocatalyst with high surface area and current response is very effective for the electrochemical degradation of textile waste.

Electrochemical degradation is one of the techniques applied in the processing of textile dyes. Additionally, its efficiency depends on factors such as the electrode material type, electrooxidation time, pH, and concentration of the electrolyte solution. This can be enhanced by employing an electrode material with a large surface area, stability, and high current response [15,21]. Incorporating an electrocatalyst into electrochemical degradation further improves the surface area, stability, and current response of the electrode material, increasing the efficiency value of the process [22].

NiO/Ni electrocatalyst is employed in the electrochemical degradation of textile waste, a treatment technique that generates highly reactive hydroxyl radicals (•OH). The hydroxyl radicals are very strong oxidizing species capable of mineralizing organic matter into carbon dioxide, water, and inorganic ions [23]. The effectiveness of electrocatalyst in the electrochemical degradation process relies on the quality of the obtained products. The quality assessment of textile waste degradation products adheres to the Indonesian Minister of Environment and Forestry Regulation No.16/MENLHK/SETJEN/KUM.1/4/2019 concerning the waste quality standards for textile industry businesses and/or activities, encompassing parameters such as COD and ammonia. The pH is a parameter that influences the formation of NiO/Ni electrocatalysts [13]. The

nickel Pourbaix diagram shows that the electrocatalytic synthesis of NiO/Ni under high pH (alkaline) conditions has a high surface area, current response, and stability characteristics. The electrocatalyst NiO/Ni is an alternative electrocatalyst with high efficiency and low production costs. The novelty of this article is the pH parameter in the electrodeposition process of the NiO/Ni affects the structure, morphology, and electrochemical properties of the NiO/Ni electrocatalyst.

Based on the described context, this study aimed to synthesize NiO/Ni electrocatalyst at various pH levels and investigate their application in the electrochemical degradation of textile wastes. The deposition of NiO/Ni electrocatalyst on graphite is expected to yield a nanocomposite structure with higher activity and stability, in comparison to graphite, during the electrochemical degradation reaction of textile waste.

2. Materials and Methods

2.1 Materials

The materials used in this study were $NiSO_4.6H_2O$ (Sigma Aldrich, > 98%), H_2O_2 (Merck, 30%), NaCl (Merck, ≥ 99.5%), H_2SO_4 (Merck, 98%), graphite electrode (SCIP, 99.9%), KOH (Merck, 85%), KCl (Merck, 99.5%), $K_2Cr_2O_7$ (Merck, 99.9%), EDTA (AR/ACS, 99.4%), NaOH (Merck, 95%), Ag_2SO_4 (Merck, 99.5%), Hg_2SO_4 (Merck, 98%), and HCl (Merck, 37-38%), and textile waste.

2.2 The Synthesis of NiO/Ni Electrocatalyst

The synthesis of the NiO/Ni electrocatalyst was conducted through Ni electrodeposition, with modifications based on the method described by Basharat *et al*. [13]. A deposition solution of 50 mL was prepared, comprising 10 mL of 0.5 M $NiSO_4.6H_2O$ solution, 5 mL of 0.1 M KOH, 4 mL of 0.4 M EDTA, and 31 mL of 0.1 M KCl as the supporting electrolyte. The pH of the deposition solution was adjusted to 8 using KOH, then stirred for 10 min at a speed of 100 rpm. Furthermore, graphite electrodes were employed as the anode and cathode, with a length of 3.5 cm immersed in the deposition solution, and a 1 cm distance between the two electrodes. The electrodeposition process was conducted at 1 volt DC power supply for 300 min at a temperature of 20–30 °C. The formed NiO/Ni electrocatalyst was subsequently heated at 400 °C for 30 min. The same procedure was repeated for the synthesis of NiO/Ni at pH of 10 and 12.

2.3 The Characterization of NiO/Ni Electrocatalyst

The morphology of the NiO/Ni electrocatalyst was characterized by scanning electron microscopy FEI Inspect-S50 (SEM-EDX) and transmission electron microscopy SAED JEOL JEM-2100 (TEM). The composition of the electrocatalyst phase was analyzed using X-ray diffraction 6000 (XRD). Additionally, the physicochemical surface properties of the NiO/Ni electrocatalyst were evaluated through N_2 adsorption-desorption measurements performed with a gas sorption analyzer (GSA) JWGB Sci and Tech Model BK112. Before analysis, the electrocatalyst was subjected to in situ pretreatment under a vacuum at 300 °C for 3 h. Subsequently, adsorption-desorption experiments were carried out using N_2 at 77.35 K. The specific surface area was determined with the multipoint BET method, while the BJH method was employed to calculate the pore size and volume. The chemical structure was confirmed with fourier transform infrared spectroscopy merk Shimadzu (FTIR). The electrocatalytic performance was determined with cyclic voltammetric Autolab type III Metrohm.

2.4 Electrochemical Degradation of Textile Waste using NiO/Ni Electrocatalyst

Textile waste was collected from household-scale textile craftsmen in the Sukawati area, Gianyar Bali. The electrochemical degradation process began by measuring the initial COD, ammonia, and pH of the textile waste. A total of 750 mL waste was adjusted to pH = 4 and supplemented with 500 mL of 0.05 M NaCl solution. The electrochemical degradation was performed using a DC power supply at 9 V for 60, 120, 180, and 240 min. Graphite electrodes coated with NiO/Ni electrocatalyst at pH = 8 were utilized as anodes, while graphite alone served as cathodes (3 pieces each). The degradation product was analyzed for absorbance, COD, and ammonia. The same procedure was repeated for NiO/Ni synthesized at pH of 10 and 12, using graphite electrodes.

The absorbance of the textile waste before and after electrochemical degradation was measured at a maximum wavelength of 595 nm with UV-vis double beam 1700 Shimadzu spectrophotometer. The efficiency of absorbance reduction in the electrochemical degradation process was calculated by Equation (1), where A_i represents the initial absorbance value, while A_f is the final value.

$$Absorbance\ reduction\ efficiency\ (\%) = \frac{A_i - A_f}{A_i} \quad (1)$$

2.5 Determination of COD Levels

COD levels were determined with closed reflux spectrophotometry, following the SNI 6989.2-2009 standard. A total of 2.5 mL sample was added to 1.5 mL of 0.0167 M $K_2Cr_2O_7$ and 3.5 mL sulfuric acid reagent solutions, then refluxed at 150 °C for 2 h. The amount of oxygen required was measured as O_2 mg.L^{-1} using a UV-vis double beam 1700 Shimadzu spectrophotometer at a wavelength of 600 nm. The COD analysis employed a UV-vis spectrophotometer with potassium hydrogen phthalate as a standard solution. The potassium hydrogen phthalate was selected as a representative organic compound in the solution, which was oxidized by potassium dichromate solution. The COD levels were calculated based on the linear equation obtained from the calibration curve of the standard solution. Moreover, the efficiency of COD reduction in the electrochemical degradation process was calculated using Equation (2), where C_i represents the initial COD level, and C_f is the final level.

$$COD\ reduction\ efficiency\ (\%) = \frac{C_i - C_f}{C_i} \quad (2)$$

2.6 Determination of Ammonia Levels

Ammonia levels were determined using a phenate spectrophotometer, following the SNI 06-6989.30-2005 standard, where the principle involved was the reaction of ammonia with hypochlorite and phenol, catalyzed by sodium nitroprusside to form an indophenol blue compound. A total of 25 mL test sample was mixed with 1 mL phenol solution, 1 mL sodium nitroprusside, and 2.5 mL sodium hypochlorite. The mixture was closed and left for 1 h before measurement with a UV-vis double beam 1700 Shimadzu spectrophotometer at a wavelength of 640 nm. The ammonia levels were calculated based on the linear equation obtained from the calibration curve. The efficiency of ammonia reduction in the electrochemical degradation process was calculated using Equation (3), where a_i represents the initial ammonia level of textile waste, and a_f is the final ammonia level.

$$Ammonia\ reduction\ efficiency\ (\%) = \frac{a_i - a_f}{a_i} \quad (3)$$

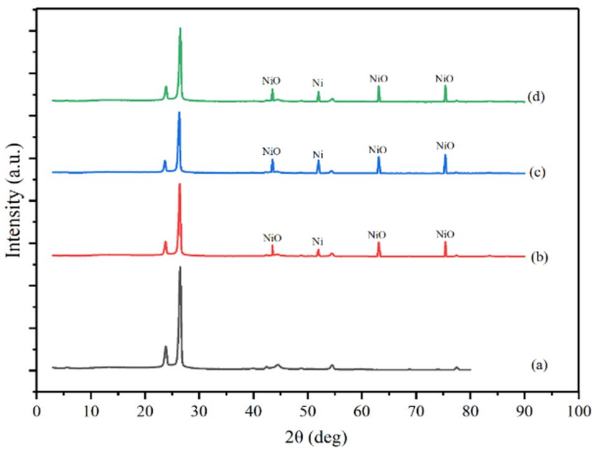

Figure 1. XRD pattern of graphite (a), NiO/Ni electrocatalyst at pH = 8 (b), NiO/Ni at pH = 10 (c), and NiO/Ni at pH = 12 (d).

3. Results and Discussion

3.1 Synthesis and Characterization of NiO/Ni Electrocatalyst

The synthesis of NiO/Ni was performed through electrodeposition, which led to the formation of green granules on the graphite electrode support material, indicating the presence of NiO and Ni electrocatalysts. The intensity of the green granules increased with higher pH values. Upon heating at 400 °C, NiO and Ni changed from green to black, indicating the ratio of Ni:O to NiO to be nonstoichiometric (the Ni:O ratio deviated from 1:1) [13].

The electrodeposition process of NiO/Ni commenced with the reduction of oxygen precursors, leading to an increase in the local pH around the cathode (Equation (4)). This was followed by the precipitation of metal oxides through electrodeposition (Equation (5)). The presence of the metal hydroxide phase could interfere with and inhibit the direct electrodeposition process of metal oxides (Equations (6) and (7)). Therefore, to convert $Ni(OH)_2$ to NiO, heating above 250 °C was required [24,25]. Ni was deposited on the surface of the graphite electrode (Equation (8)) due to the greater standard reduction potential of Ni^{2+} to Ni ($E°$ = −0.257 V/SHE) compared to the standard reduction potential of H_2O to OH^- ($E°$ = −0.828 V/SHE) [17].

$$O_2 + 2\ H_2O + 4e^- \rightarrow 4OH^- \quad (4)$$
$$M^{n+} + nOH^- \rightarrow M(OH)_n \rightarrow MO_{n/2} + n/2\ H_2O \quad (5)$$
$$O_2 + 4\ e^- \rightarrow 2O^{2-} \quad (6)$$
$$Ni^{2+} + O^{2-} \rightarrow NO + ½\ O_2 \quad (7)$$
$$Ni^{2+} + 2e^- \rightarrow Ni \quad (8)$$

To prevent the precipitation of Ni^{2+} into $Ni(OH)_2$ during the electrodeposition process carried out at alkaline conditions (pH of 8, 10,

and 12), EDTA was added to the reaction mixture. The addition of EDTA hindered the formation of $Ni(OH)_2$, facilitating easier direct deposition of metal oxides. The formation of the Ni-EDTA complex was indicated by a color change in the deposition solution from green to blue [13].

The composition of NiO/Ni electrocatalyst surface phase was determined through XRD analysis. Figure 1 shows the diffractograms of graphite, as well as NiO/Ni, synthesized at pH of 8, 10, and 12. The characteristic peaks at $2\theta = 26.5°$ (002) and $2\theta = 54.6°$ (004) corresponded to graphite [26]. Furthermore, the XRD diffractogram of NiO/Ni revealed the emergence of four new diffraction peaks at $2\theta = 43.5°$, 51.9°, 63.1°, and 75.4°. These peaks indicated the presence of NiO deposited on graphite at $2\theta = 43.5°$, 63.1°, and 75.4°, while the peak at $2\theta = 51.9°$ correlated with the characteristics of Ni (JCPDS No. 70-0989) [27]. Therefore, it could be concluded that NiO/Ni electrocatalyst was successfully deposited on the graphite electrode.

Figure 2 shows the SEM results of graphite, as well as NiO/Ni, synthesized at pH of 8, 10, and 12, which were observed at 5 μm magnification. The SEM images reveal the deposition of the electrocatalyst onto the graphite surface. The SEM image of graphite in Figure 2(a) shows a plain surface, while the images in Figures 2(b), (c), and (d) display the granular, spherical, solid, flake, and cracked structures of NiO/Ni. These morphological variations indicated the formation of NiO/Ni on the graphite surface. The SEM analysis revealed an interesting trend regarding the influence of pH on the morphology of NiO/Ni electrocatalyst. With an increase in pH, the presence of flake-like structures decreased, while the occurrence of granular, spherical, solid, and fractured structures increased. This observation suggested that the formation of NiO/Ni was more pronounced at higher pH values. The NiO/Ni synthesized at pH = 12 (Figure 2(d)) exhibited granular, spherical, and increased crack features. The granular morphology indicated a

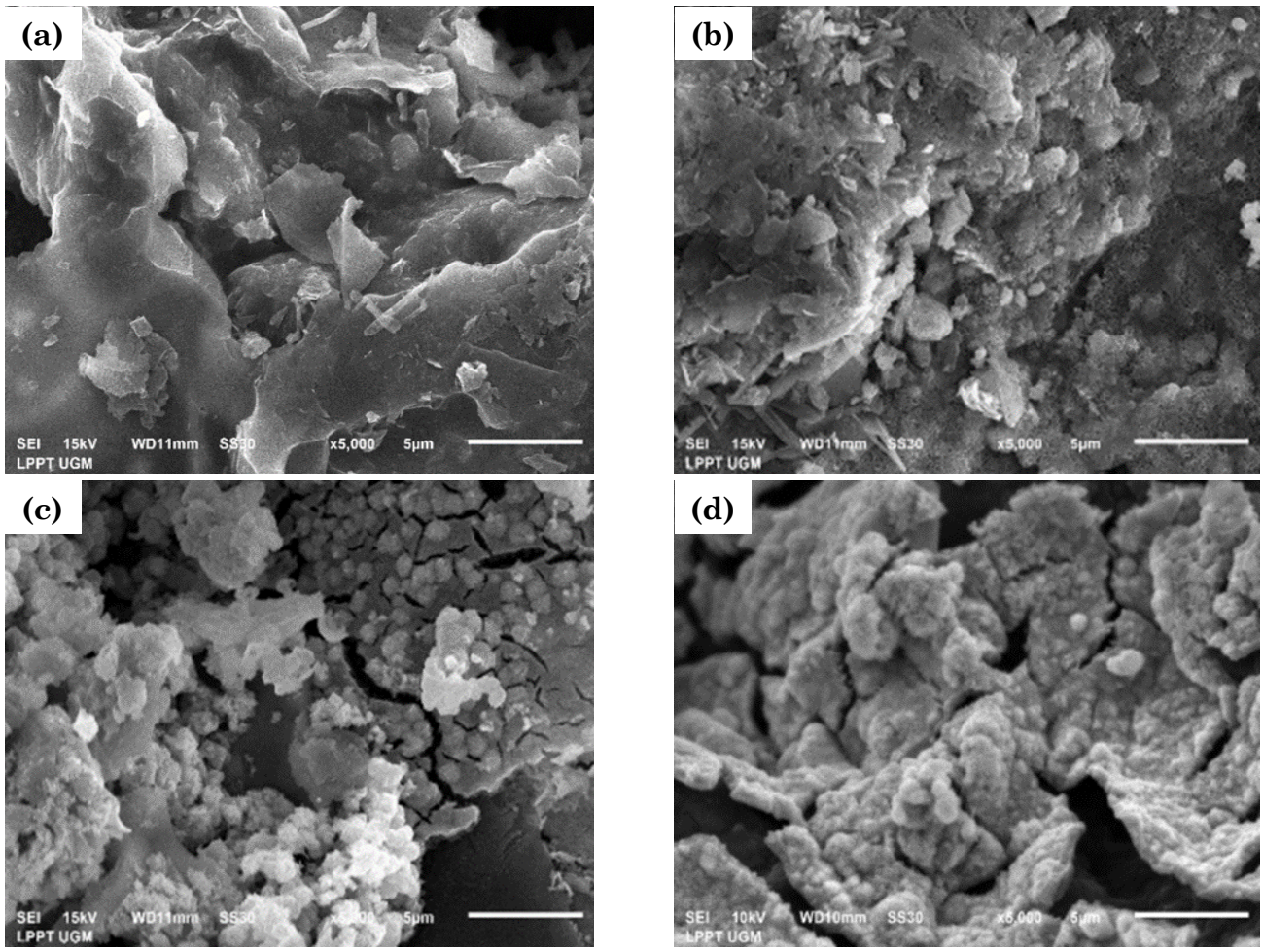

Figure 2. SEM images of graphite (a), NiO/Ni electrocatalyst at pH = 8 (b), NiO/Ni at pH = 10 (c), and NiO/Ni at pH = 12 (d).

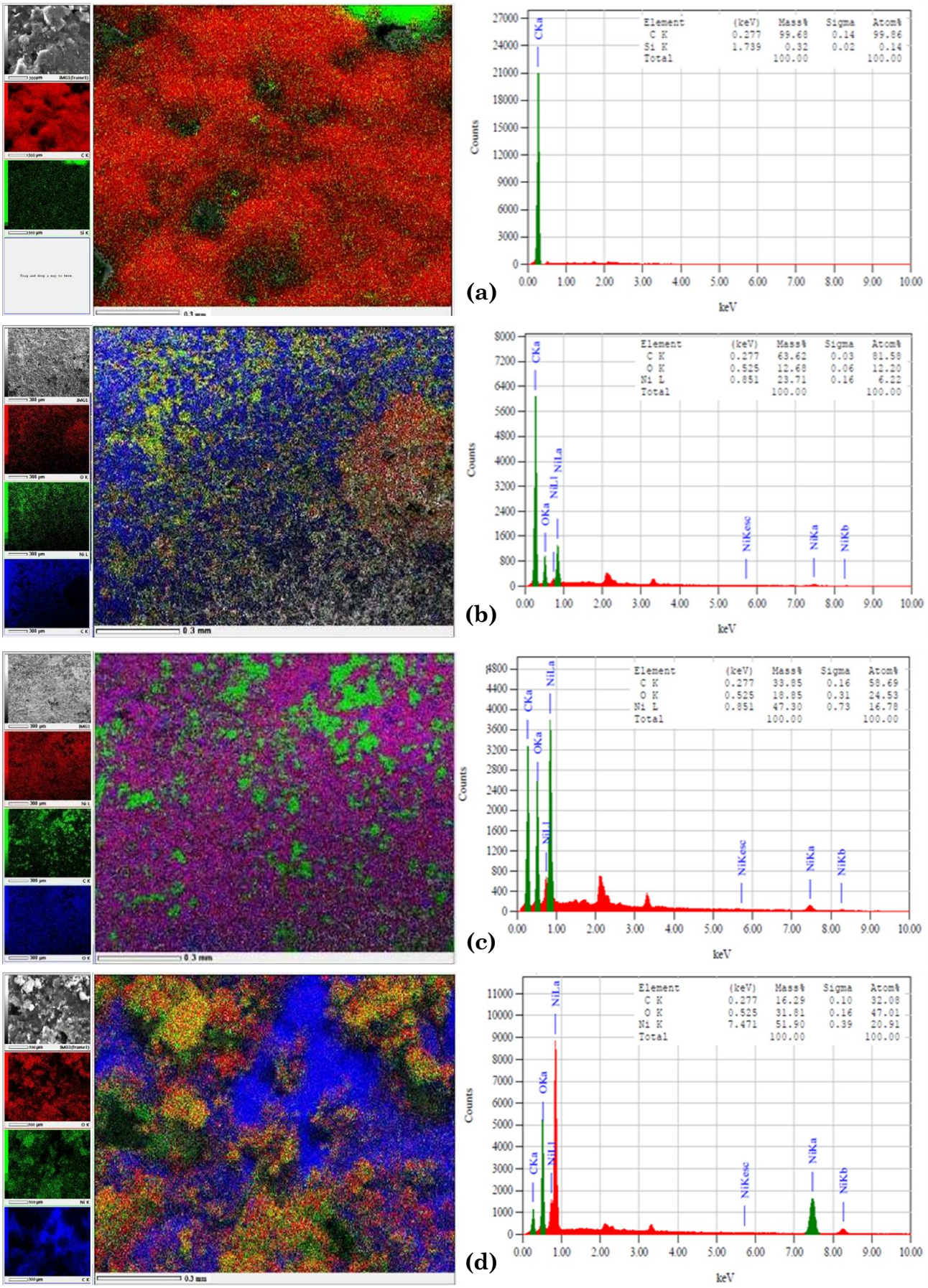

Figure 3. EDX spectrum of graphite (a), NiO/Ni at pH = 8 (b), NiO/Ni electrocatalyst at pH = 10 (c), and NiO/Ni at pH = 12 (d).

large surface area, while the presence of cracks was associated with contraction induced by tensile stress during drying [13,28].

To further confirm the presence of NiO/Ni on the graphite surface, energy-dispersive X-ray (EDX) mapping was performed, and the results provided spatial information about the elemental composition of the electrocatalyst. According to Figure 3(a), the dominant elements detected on the graphite surface were carbon, along with a small amount of silicon (0.14%). In Figure 3(b), the NiO/Ni deposition appeared less evenly distributed, indicating a lower amount of NiO/Ni formed at pH = 8. Figure 3(c) shows a more uniform distribution of NiO/Ni, suggesting an increased formation of NiO/Ni at pH = 10. Figure 3(d) reveals a thick layer of NiO/Ni deposited on a specific edge of the graphite surface. These EDX mapping results align with previous studies that reported the even distribution of Ni/SiO_2 nanocomposites on Cu electrodes synthesized through electrodeposition [29].

EDX analysis was employed to confirm the presence of Ni and O particles scattered on the graphite surface, and the results are presented in Figure 3. Interestingly, the proportion of Ni and O in NiO/Ni synthesized at pH = 12 was found to be the highest compared to the other electrocatalysts. This observation aligned with the Pourbaix diagram of nickel, which indicated the formation of NiO at pH of 8–13. Besides, more $Ni(OH)_2$ was possibly formed at pH = 12, suggesting the reason behind the thick and congregated layer observed in the SEM image (Figure 2(d)).

The FTIR spectra of graphite and the three NiO/Ni electrocatalysts in the wave number range of 500–4000 cm^{-1} presented in Figure 4 provided valuable information about their chemical composition. The FTIR spectra of NiO/Ni in Figures 4(b), (c), and (d) showed that a peak at wave number 700 cm^{-1}, 501 cm^{-1}, and 1635 cm^{-1} corresponded to the stretching vibrations of Ni^{2+}–OH [3], Ni–O [30], and H–O–H [31], respectively. In contrast, the FTIR spectrum of graphite (Figure 4(a)) did not exhibit these characteristic peaks.

The specific surface area characterization in Figure 5 revealed a type (IV) adsorption/desorption isotherm curve according to IUPAC classification, with a hysteresis loop at relatively high pressure. This behavior indicated the occurrence of capillary condensation in mesoporous materials [12,32]. Figure 5 shows that NiO/Ni synthesized at pH = 10 exhibited the highest potential for the electrochemical degradation of textile waste. The pore size distribution of graphite and the electrocatalyst

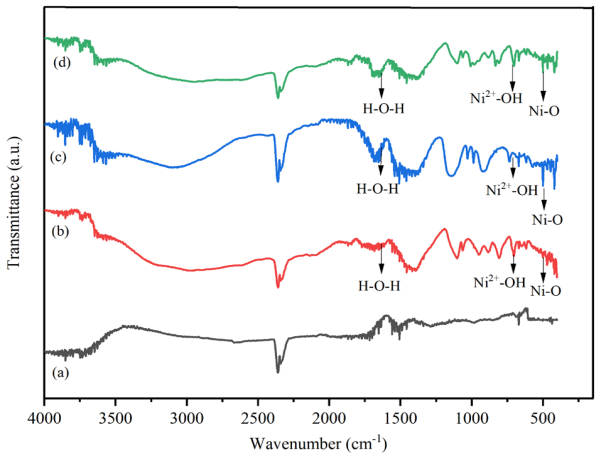

Figure 4. FTIR spectrum of graphite (a), NiO/Ni at pH = 8 (b), NiO/Ni at pH = 10 (c), and NiO/Ni at pH = 12 (d).

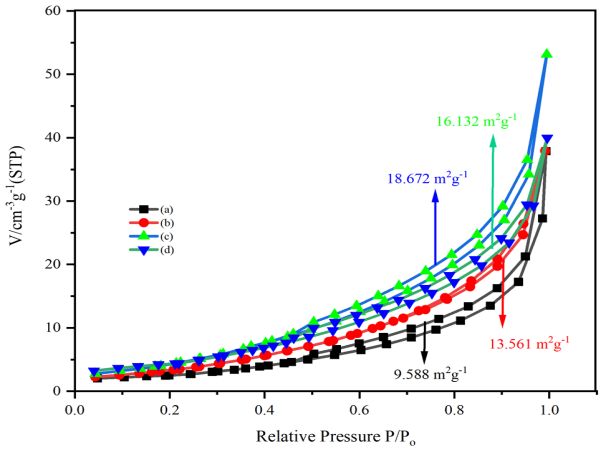

Figure 5. The nitrogen adsorption-desorption isotherms of graphite (a), NiO/Ni electrocatalyst at pH = 8 (b), NiO/Ni at pH = 10 (c), and NiO/Ni at pH = 12 (d).

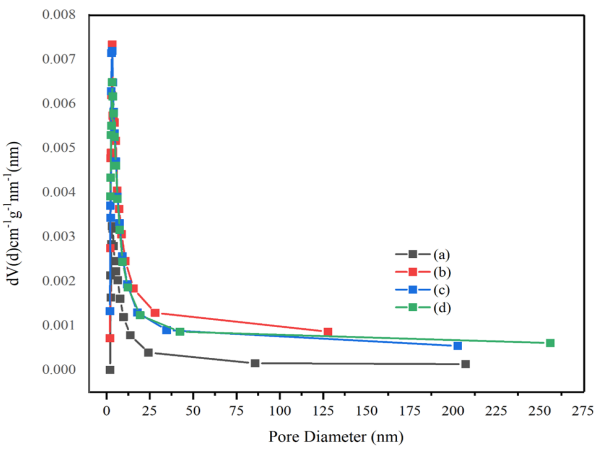

Figure 6. The pore diameter distributions of graphite (a), NiO/Ni at pH = 8 (b), NiO/Ni at pH = 10 (c), and NiO/Ni at pH = 12 (d).

NiO/Ni was determined using the BJH model, as indicated in Figure 6. Both graphite and NiO/Ni are mesoporous materials, with a relatively uniform pore size distribution ranging from 2 to 25 nm. Notably, NiO/Ni at pH = 10 (0.079 cm^3/g) had the highest pore volume compared to graphite (0.052 cm^3/g), as well as NiO/Ni at pH = 8 (0.058 cm^3/g) and pH = 12 (0.059 cm^3/g), which was greatly advantageous for the electrochemical degradation of textile waste. A larger specific surface area and pore volume contribute to enhanced catalytic activity in the electro-oxidation of hydrogen peroxide [33]. A previous study reported the synthesis of NiO@Si nanocomposite anodes using the impregnation method, leading to increased surface area and pore volume, while the pore diameter decreased with the progressive deposition of NiO nanocomposite on Si [12]. Additionally, the impregnation of Cu onto Ni/ZrO_2 catalyst yielded a significant increase in the specific surface area as measured by the BET method, along with a decrease in the pore diameter. This effect could be attributed to potential blockage of the porosity of the support material by the added Cu [34].

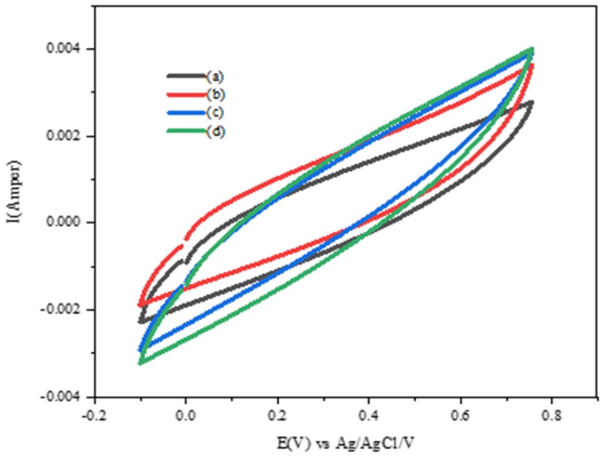

Figure 7. Voltamogram of of graphite (a), NiO/Ni at pH = 8 (b), NiO/Ni at pH = 10 (c), and NiO/Ni at pH = 12, (d) as well as 0.1 M NaCl and scan rate of 10 $mV.s^{-1}$.

Figure 7 shows the voltammogram of graphite and NiO/Ni electrocatalyst. The high current response observed in the voltammogram indicated the enhanced activity for the Cl^- oxidation reaction [35,36]. Notably, the current response of NiO/Ni deposited on graphite was

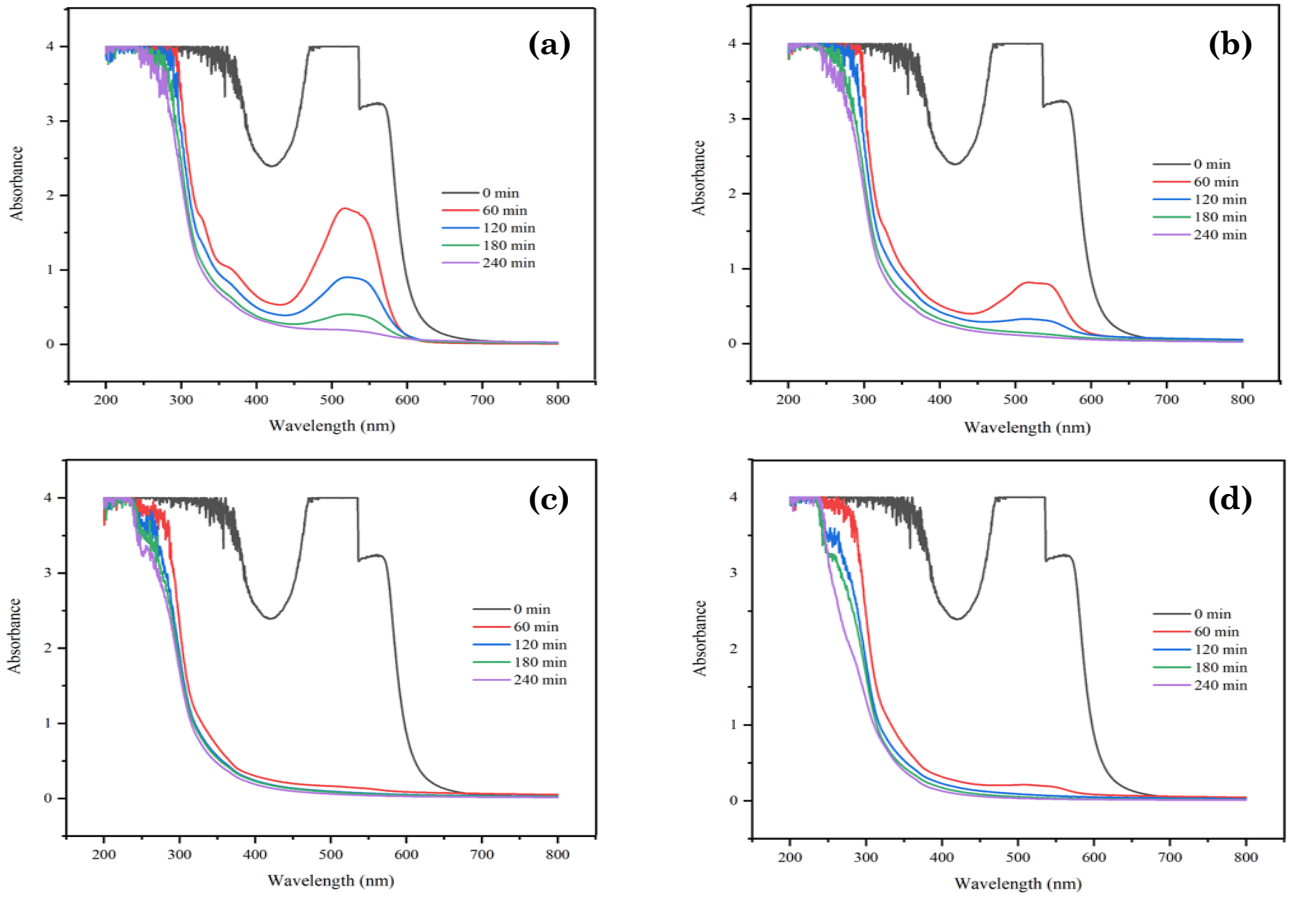

Figure 8. The absorbance spectra of graphite (a), NiO/Ni at pH = 8 (b), NiO/Ni at pH = 10 (c), and NiO/Ni at pH = 12 (d).

higher than that of pure graphite, indicating superior electrocatalytic activity.

3.2 Electrochemical Degradation of Textile Waste

The textile waste used for the electrochemical degradation process was collected from household-scale textile craftsmen located in the Sukawati area of Gianyar Bali. This waste comprised a mixture of organic and inorganic materials, including remazol red and black dyes, with COD of 2,400.833 $mg.L^{-1}$, ammonia content of 95.288 $mg.L^{-1}$, and a pH of 12.

In electrolytic cells, the electrochemical degradation of organic pollutants occurs through two primary mechanisms, namely direct anodic oxidation and indirect oxidation [37]. Direct electrochemical degradation of textile waste is often carried out using hydroxyl radicals or by direct electron transfer to the anode, as presented in Equations (9)–(11). On the other hand, the indirect process involves the generation of active chlorine species from chloride ions at the anode to degrade textile waste, as illustrated in Equation (10) [38,39].

$$M + H_2O \rightarrow M(\bullet OH) \quad (9)$$

$$M(\bullet OH) + \text{textile waste} \rightarrow M + \text{intermediate} \quad (10)$$

$$M(\bullet OH) + \text{intermediate} \rightarrow M + CO_2 + H_2O + \text{inorganic ion} \quad (11)$$

$$\text{Textile waste} + HOCl \rightarrow CO_2 + H_2O + Cl^- \quad (12)$$

These electrochemical degradation pathways play a crucial role in the breakdown of the textile waste components, leading to the eventual conversion into CO_2, H_2O, and inorganic ions.

Figure 8 shows the spectra of textile waste before and after the electrochemical degradation process. Furthermore, it displays a prominent peak in the visible region (400–600 nm), indicating the presence of the azo chromophore group (−N=N−). Another peak found in the UV region (200–400 nm) represents unsaturated groups, such as benzene, naphthalenes, and heterocyclic rings [40–42]. During the electrochemical degradation conducted using graphite and NiO/Ni at pH = 8, a reduction in peaks within the visible region was observed. Meanwhile, in the degradation process involving NiO/Ni synthesized at pH of 10 and 12, a significant decrease and even disappearance of the peaks occurred. These results suggested that the chromophore groups turned into intermediates before the formation of aliphatic carboxylic acids and carbon dioxide. The described transformation events accelerated the decline in absorbance and disappearance of the visible peaks [41]. The absorbance decrease in the UV region was less pronounced compared to the visible region because the aromatic structures of compounds found in the textile waste were more stable than the azo chromophore group [42].

Figure 9(a) shows that as the electrochemical degradation process continues, the absorbance reduction efficiency of the textile waste

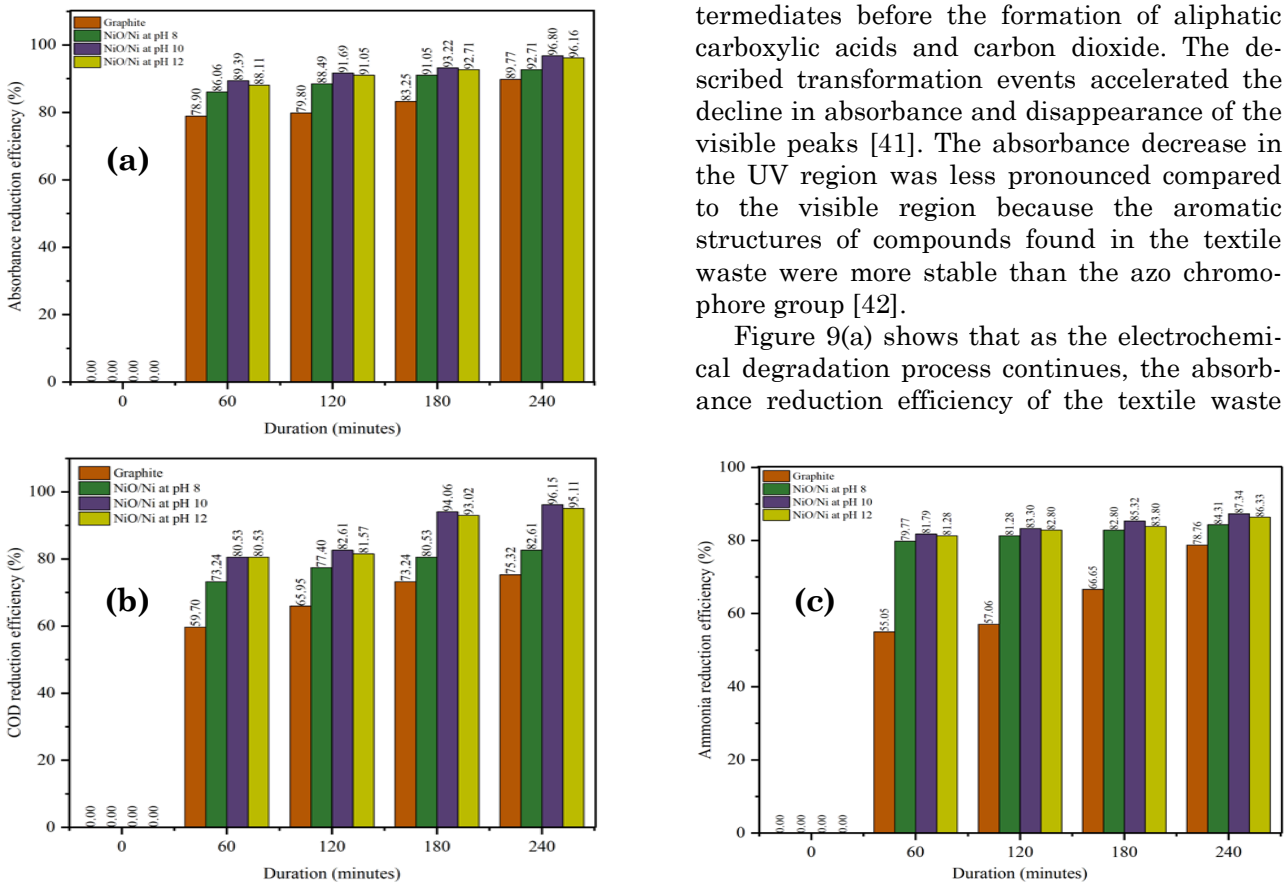

Figure 9. The relation between reduction efficiencies of absorbance (a), COD (b), and ammonia (c) with duration.

increases. This can be attributed to the extended contact between chlorine species or hydroxyl radicals and the textile waste, leading to enhanced generation of degradation products [43,44]. In this study, after 240 min of the electrochemical degradation process, the highest absorbance reduction efficiencies were 89.77%, 92.71%, 96.80%, and 96.61% for graphite, as well as NiO/Ni synthesized at pH of 8, 10, and 12.

The efficiency of reducing COD presented in Figure 9(b) indicates that as the electrochemical degradation process prolongs, the reduction in COD becomes more significant. For graphite, the reduction efficiency increased from 59.70% after 60 min of processing to 75.32% after 240 min. Similarly, when using NiO/Ni synthesized at pH of 8, 10, and 12, the efficiency improved from 73.24–82.61%, 80.53–96.15%, and 80.53–95.11%, respectively. These results aligned with a previous study that stated a consistent increase in COD removal efficiency along with longer electrochemical degradation processes.

Several previous studies examined the electrooxidation and electrodegradation of textile waste, yielding significant insights. For instance, the electrooxidation of textile waste with an initial COD of 1,075 $mg.L^{-1}$, using a G/β-PbO_2 anode, which achieved a COD removal efficiency of 62.3% [45]. Electrooxidation with a BDD anode at pH 2, a current strength of 60 $mA.cm^{-2}$, and a NaCl concentration of 3 $mg.L^{-1}$, the result showed that the longer the electrooxidation process, the higher the removal efficiency, reaching 95% after 6 h of processing for textile waste with an initial COD of 2,154 $mg.L^{-1}$ [46]. In a separate investigation, the electrodegradation was performed using a Ti/β-PbO_2 anode under conditions of 5.6 V, 4000 $mg.L^{-1}$ NaCl concentration, and pH 6. After 4 h of processing, this approach reduced COD by 59% and NH_3 by 74% [36]. Additionally, an electrocatalytic treatment that employed DSA Ti/RuO_2 electrodes showed a COD reduction of 86.22% and a 94.74% reduction in textile color after 124 min of processing at pH 5.54 and a strong current of 1.37 A [23].

The electrochemical degradation of ammonia is carried out through direct and indirect anodic mechanisms. In the direct electrochemical degradation, the pollutant is oxidized after being transferred to the anode surface (Equation (13)), while the indirect degradation occurs in the presence of active chlorine oxidizing agents such as Cl_2, HOCl, and OCl^- (Equations (14) and (15)).

$$2NH_4^+ + 6 \cdot OH \rightarrow N_2 + 6H_2O \quad (13)$$

$$2NH_4^+ + 3HClO \rightarrow N_2 + 3H_2O + 5H^+ + 3Cl^- \quad (14)$$

$$NH_4^+ + 4HClO \rightarrow NO_3^- + H_2O + 6H^+ + 4Cl^- \quad (15)$$

According to Figure 9(c), the electrochemical degradation time and ammonia reduction efficiency increase simultaneously. This can be attributed to the larger number of active hydroxyl radicals and chlorine species generated during the process, facilitating efficient degradation of ammonia, as indicated in Equations (9)–(11) [47–49]. In a study using RuO_2-IrO_2-TiO_2/Ti electrodes, ammonia concentration decreased linearly with increasing time from 515 to 0.1 $mg.L^{-1}$ after 2 h of degradation [50].

The electrochemical degradation process conducted for 240 min yielded the following highest ammonia reduction efficiencies of 78.76, 84.31, 87.34, and 86.33% for graphite, as well as NiO/Ni electrocatalyst, synthesized at pH of 8, 10, and 12, respectively. Previous studies reported that a Ti/PbO_2 anode achieved 95% conversion of ammonia to nitrogen (N_2) at pH 5 in wastewater, with only 4.83% converting to NO_3 within 120 min of electrolysis [48]. Moreover, N-Doped ZnO Beads (N-ZnB) at pH = 6.19 degraded ammonia by 95.75% after 2 h of processing [51].

The reduction efficiency absorbance, COD, and ammonia of the NiO/Ni pH = 10 electrocatalyst was the highest compared to the others, due to the electrodeposition of the NiO/Ni pH = 10 on the surface graphite electrode which can improve the surface area and current respond (Figures 1-7), so improve electrooxidation performance of textile waste. After 240 min of electrochemical degradation, the COD content of textile waste was measured as 592.5, 417.5, 92.5, and 117.5 $mg.L^{-1}$ for graphite, as well as NiO/Ni synthesized at pH of 8, 10, and 12, respectively. Furthermore, the ammonia content after the same degradation time was 20.240, 14.952, 12.067, and 13.029 $mg.L^{-1}$ for graphite and the three electrocatalysts, respectively. Based on the COD levels achieved after 240 min of electrooxidation, it can be concluded that the electrochemical degradation products generated using NiO/Ni synthesized at pH of 10 and 12 enable the safe disposal of textile waste into the environment, adhering to the waste quality standards defined by the Regulation of the Indonesian Minister of Environment and Forestry No P. 16/MENLHK/SETJEN/KUM.1/4/2019.

4. Conclusions

In conclusion, this study successfully synthesized NiO/Ni electrocatalyst through electrodeposition at pH of 8, 10, and 12, as confirmed by XRD, FTIR, and SEM-EDX spectra. Moreover, NiO/Ni electrocatalysts synthesized at pH = 10 exhibited the highest surface area, pore volume, and current response compared to graphite and other electrocatalysts. The optimal conditions for the electrochemical degradation of textile waste at pH = 4, 0.05 M NaCl, 9 volts, and a processing time of 240 min. The highest reduction efficiencies achieved for absorbance, COD, and ammonia using the NiO/Ni electrocatalyst at pH = 10 were 96.80, 96.15, and 87.34%, respectively. Meanwhile, the lowest reduction efficiencies were 78.90, 59.70, and 55.05% respectively, which were obtained using graphite. These results highlighted the great potential of the NiO/Ni electrocatalyst pH = 10 for textile waste degradation.

Acknowledgment

This research was supported by Chemistry Department, FMIPA, Universitas Pendidikan Ganesha.

Credit Author Statement

Ni Made Wiratini: Conceptualization, Methodology, Investigation, Resources, Data Curation, Writing, Review and Editing. All authors have read and agreed to the published version of the manuscript.

References

[1] Patel, P.S., Bandre, N., Saraf, A., Ruparelia, J.P. (2013). Electro-Catalytic Materials (Electrode Materials) in Electrochemical Wastewater Treatment. *Procedia Engineering*, 51, 430–435. DOI: 10.1016/j.proeng.2013.01.060.

[2] Jaksic, M.M., Schmickleer, W., Botton, G. (2012). Advances in Electrocatalysis. *Advances in Physical Chemistry*, 2012, 180604. DOI: 10.1155/2012/180604.

[3] Jinisha, R., Gandhimathi, R., Ramesh, S.T., Nidheesh, P. V., Velmathi, S. (2018). Removal of Rhodamine B Dye from Aqueous Solution by Electro-Fenton Process Using Iron-doped Mesoporous Silica as a Heterogeneous Catalyst. *Chemosphere*, 200, 446–454. DOI: 10.1016/j.chemosphere.2018.02.117.

[4] Döner, A., Telli, E., Kardaş, G. (2012). Electrocatalysis of Ni-Promoted Cd Coated Graphite Toward Methanol Oxidation in Alkaline Medium. *Journal of Power Sources*, 205, 71–79. DOI: 10.1016/j.jpowsour.2012.01.020.

[5] Ding, R., Li, X., Shi, W., Xu, Q., Wang, L., Jiang, H., Yang, Z., Liu, E. (2016). Mesoporous Ni-P Nanocatalysts for Alkaline Urea Electrooxidation. *Electrochimica Acta*, 222, 455–462. DOI: 10.1016/j.electacta.2016.10.198.

[6] Alotaibi, R., Alenazey, F., Alotaibi, F., Wei, N., Al-Fatesh, A., Fakeeha, A. (2015). Ni Catalysts with Different Promoters Supported on Zeolite for Dry Reforming of Methane. *Applied Petrochemical Research*, 5(4), 329–337. DOI: 10.1007/s13203-015-0117-y.

[7] Kannan, R., Govindan, K., Selvaraj, S., Ravichandiran, P., Vasanthkumar, S. (2013). Birnessite Nanorod-mediated Decomposition of Methylene Blue with Common Oxidants. *Applied Water Science*, 3(1), 335–341. DOI: 10.1007/s13201-012-0058-x.

[8] Ahmed, J., Ahamad, T., Al Shehri, S.M. (2017). Iron–Nickel Nanoparticles as Bifunctional Catalysts in Water Electrolysis. *Chemelectrochem*, 4(5), 1222–1226. DOI: 10.1002/celc.201600754.

[9] He, S., Zhang, L., He, S., Mo, L., Zheng, X., Wang, H., Luo, Y. (2015). Ni/SiO_2 Catalyst Prepared with Nickel Nitrate Precursor for Combination of CO_2 Reforming and Partial Oxidation of Methane: Characterization and Deactivation Mechanism Investigation. *Journal of Nanomaterials*, 2015, 659402. DOI: 10.1155/2015/659402

[10] Feng, Z., Wang, L., Li, D., Sun, Q., Xing, P., An, M. (2019). Electrochemical Studies of 2-Aminopyridine on Nanocrystalline Zn–Ni Alloy Electrodeposition. *Journal of Electroanalytical Chemistry*, 835, 114–122. DOI: 10.1016/j.jelechem.2019.01.038.

[11] Yan, W., Wang, D., Botte, G.G. (2012). Electrochemical Decomposition of Urea with Ni-Based Catalysts. *Applied Catalysis B: Environmental*, 127, 221–226. DOI: 10.1016/j.apcatb.2012.08.022.

[12] Kawade, U.V., Kadam, S.R., Kulkarni, M.V., Kale, B.B. (2020). Synergic Effects of the Decoration of Nickel Oxide Nanoparticles on Silicon for Enhanced Electrochemical Performance in LIBs. *Nanoscale Advances*, 2(2), 823–832. DOI: 10.1039/c9na00727j.

[13] Basharat, F., Rana, U.A., Shahid, M., Serwar, M. (2015). Heat Treatment of Electrodeposited NiO Films for Improved Catalytic Water Oxidation. *RSC Advances*, 5(105), 86713–86722. DOI: 10.1039/c5ra17041a.

[14] Sonavane, A.C., Inamdar, A.I., Shinde, P.S., Deshmukh, H.P., Patil, R.S., Patil, P.S. (2010). Efficient Electrochromic Nickel Oxide Thin Films by Electrodeposition. *Journal of Alloys and Compounds*, 489(2), 667–673. DOI: 10.1016/j.jallcom.2009.09.146.

[15] Shestakova, M., Sillanpää, M. (2017). Electrode Materials Used for Electrochemical Oxidation of Organic Compounds in Wastewater. *Reviews in Environmental Science and Biotechnology*, 16(2), 223–238. DOI: 10.1007/s11157-017-9426-1.

[16] Ijeh, R.O., Nwanya, A.C., Nkele, A.C., Madiba, I.G., Khumalo, Z., Bashir, A.K.H., Osuji, R.U., Maaza, M., Ezema, F.I. (2019). Magnetic and Optical Properties of Electrodeposited Nanospherical Copper Doped Nickel Oxide Thin Films. *Physica E: Low-Dimensional Systems and Nanostructures*, 113, 233–239. DOI: 10.1016/j.physe.2019.05.013.

[17] Bard, A.J., Faulkner, L.R. (2001). *Electrochemical Methods Fundamentals and Application*.

[18] Trasatti, S. (1992). Adsorption of Organic Substances at Electrodes: Recent Advances. *Electrochimica Acta*, 37(12), 2137–2144. DOI: 10.1016/0013-4686(92)85104-S.

[19] Huang, L.F., Hutchison, M.J., Santucci, R.J., Scully, J.R., Rondinelli, J.M. (2017). Improved Electrochemical Phase Diagrams from Theory and Experiment: The Ni-Water System and Its Complex Compounds. *Journal of Physical Chemistry C*, 121(18), 9782–9789. DOI: 10.1021/acs.jpcc.7b02771.

[20] Huang, L.-F., Rondinelli, J.M. (2019). Reliable Electrochemical Phase Diagrams of Magnetic Transition Metals and Related Compounds from High-Throughput AB Initio Calculations. *npj Materials Degradation*, 3(1), 26. DOI: 10.1038/s41529-019-0088-z.

[21] Ajeel, M.A., Aroua, M.K., Daud, W.M.A.W. (2015). Anodic Degradation of 2-Chlorophenol by Carbon Black Diamond and Activated Carbon Composite Electrodes. *Electrochimica Acta*, 180, 22–28. DOI: 10.1016/j.electacta.2015.08.062.

[22] Mukimin, A., Wijaya, K., Kuncaka, A. (2010). Electrodegradation of Reactive Blue Dyes Using Cylinder Modified Electrode: Ti/ß-PbO_2 as Dimensionally Stable Anode. *Indonesian Journal of Chemistry*, 10(3), 285–289. DOI: 10.22146/ijc.21431.

[23] Kaur, P., Kushwaha, J.P., Sangal, V.K. (2018). Electrocatalytic Oxidative Treatment of Real Textile Wastewater in Continuous Reactor: Degradation Pathway and Disposability Study. *Journal of Hazardous Materials*, 346, 242–252. DOI: 10.1016/j.jhazmat.2017.12.044.

[24] Azaceta, E., Chavhan, S., Rossi, P., Paderi, M., Fantini, S., Ungureanu, M., Miguel, O., Grande, H.J., Tena-Zaera, R. (2012). NiO Cathodic Electrochemical Deposition from an Aprotic Ionic Liquid: Building Metal Oxide N-P Heterojunctions. *Electrochimica Acta*, 71, 39–43. DOI: 10.1016/j.electacta.2012.03.093.

[25] Koussi-Daoud, S., Majerus, O., Schaming, D., Pauporté, T. (2016). Electrodeposition of NiO Films and Inverse Opal Organized Layers from Polar Aprotic Solvent-Based Electrolyte. *Electrochimica Acta*, 219, 638–646. DOI: 10.1016/j.electacta.2016.10.074.

[26] Popova, A.N. (2017). Crystallographic Analysis of Graphite by X-Ray Diffraction. *Coke and Chemistry*, 60(9), 361–365. DOI: 10.3103/S1068364X17090058.

[27] Fan, M., Ren, B., Yang, X., Yu, H., Wang, L. (2019). NiO@NiO and NiO@Co 3 O 4 Hollow Core/Shell Composites for High-Performance Supercapacitor Electrodes. *Journal of Nanoscience and Nanotechnology*, 19(12), 7785–7789. DOI: 10.1166/jnn.2019.16857.

[28] Kim, H.B., Kim, H., Sohn, H.S., Son, I., Lee, H.S. (2013). Effect of pH on the Morphological Evolution of NiO Thin Film Synthesized on ZnO Nanorod Arrays by Electrodeposition and Post-Annealing. *Materials Letters*, 101, 65–68. DOI: 10.1016/j.matlet.2013.03.077.

[29] Li, R., Hou, Y., Liu, B., Wang, D., Liang, J. (2016). Electrodeposition of Homogenous Ni/SiO_2 Nanocomposite Coatings from Deep Eutectic Solvent with In-situ Synthesized SiO_2 Nanoparticles. *Electrochimica Acta*, 222, 1272–1280. DOI: 10.1016/j.electacta.2016.11.101.

[30] Rebelo, Q.H.F., Ferreira, C.S., Santos, P.L., Bonacin, J.A., Passos, R.R., Pocrifka, L.A., Paula, M.M.S. (2019). Synthesis and Characterization of a Nanocomposite NiO/SiO_2 from a Sustainable Source of SiO_2. *Particulate Science and Technology*, 37(8), 907–911. DOI: 10.1080/02726351.2018.1455781.

[31] Krishnakumar, B., Kumar, S., Gil, J.M., Mani, D., Arivanandhan, M., Sobral, A.J.F.N. (2019). Synthesis and Characterization of g/Ni–SiO_2 Composite for Enhanced Hydrogen Storage Applications. *International Journal of Hydrogen Energy*, 44(41), 23249–23256. DOI: 10.1016/j.ijhydene.2019.07.073.

[32] Liang, K., Tang, X., Hu, W. (2012). High-Performance Three-Dimensional Nanoporous NiO Film as a Supercapacitor Electrode. *Journal of Materials Chemistry*, 22(22), 11062–11067. DOI: 10.1039/c2jm31526b.

[33] Zhang, J., Zhang, D., Liu, Y. (2019). Ni–SiO_2 Nanoporous Composite as an Efficient Electrocatalyst for the Electrooxidation of Hydrogen Peroxide. *Journal of Materials Science: Materials in Electronics*, 30(15), 13895–13909. DOI: 10.1007/s10854-019-01707-0.

[34] Zhang, X., Wang, T., Ma, L., Zhang, Q., Yu, Y., Liu, Q. (2013). Characterization and Catalytic Properties of Ni and NiCu Catalysts Supported on ZrO_2-SiO_2 for Quaiacol Hydrodeoxygenation. *Catalysis Communications*, 33, 15–19. DOI: 10.1016/j.catcom.2012.12.011.

[35] Bi, Q., Guan, W., Gao, Y., Cui, Y., Ma, S., Xue, J. (2019). Study of The Mechanisms Underlying The Effects of Composite Intermediate Layers on The Performance of Ti/SnO_2-Sb-La Electrodes. *Electrochimica Acta*, 306, 667–679. DOI: 10.1016/j.electacta.2019.03.122.

[36] Mukimin, A., Vistanty, H., Zen, N. (2015). Oxidation of Textile Wastewater Using Cylinder Ti/ß-PbO_2 Electrode in Electrocatalytic Tube Reactor. *Chemical Engineering Journal*, 259, 430–437. DOI: 10.1016/j.cej.2014.08.020.

[37] Garcia-Segura, S., Ocon, J.D., Chong, M.N. (2018). Electrochemical oxidation remediation of real wastewater effluents — A review. *Process Safety and Environmental Protection*, 113, 48–67. DOI: 10.1016/j.psep.2017.09.014.

[38] Särkkä, H., Bhatnagar, A., Sillanpää, M. (2015). Recent developments of electro-oxidation in water treatment - A review. *Journal of Electroanalytical Chemistry*, 754, 46–56. DOI: 10.1016/j.jelechem.2015.06.016.

[39] Samarghandi, M.R., Dargahi, A., Shabanloo, A., Nasab, H.Z., Vaziri, Y., Ansari, A. (2020). Electrochemical Degradation of Methylene Blue Dye Using a Graphite Doped PbO_2 Anode: Optimization of Operational Parameters, Degradation Pathway and Improving the Biodegradability of Textile Wastewater. *Arabian Journal of Chemistry*, 13(8), 6847–6864. DOI: 10.1016/j.arabjc.2020.06.038.

[40] Droguett, T., Mora-Gómez, J., García-Gabaldón, M., Ortega, E., Mestre, S., Cifuentes, G., Pérez-Herranz, V. (2020). Electrochemical Degradation of Reactive Black 5 Using Two-different Reactor Configuration. *Scientific Reports*, 10(1), 1–11. DOI: 10.1038/s41598-020-61501-5.

[41] Rivera, M., Pazos, M., Sanromán, M.Á. (2011). Development of an Electrochemical Cell for The Removal of Reactive Black 5. *Desalination*, 274(1–3), 39–43. DOI: 10.1016/j.desal.2011.01.074.

[42] Tang, Y., He, D., Guo, Y., Qu, W., Shang, J., Zhou, L., Pan, R., Dong, W. (2020). Electrochemical Oxidative Degradation of X-6G Dye by Boron-Doped Diamond Anodes: Effect of Operating Parameters. *Chemosphere*, 258, 127368. DOI: 10.1016/j.chemosphere.2020.127368.

[43] Basha, C.A., Sendhil, J., Selvakumar, K. V., Muniswaran, P.K.A., Lee, C.W. (2012). Electrochemical Degradation of Textile Dyeing Industry Effluent in Batch and Flow Reactor Systems. *Desalination*, 285, 188–197. DOI: 10.1016/j.desal.2011.09.054.

[44] Najafpoor, A.A., Davoudi, M., Rahmanpour Salmani, E. (2017). Decolorization of Synthetic Textile Wastewater Using Electrochemical Cell Divided by Cellulosic Separator. *Journal of Environmental Health Science and Engineering*, 15(1), 1–11. DOI: 10.1186/s40201-017-0273-3.

[45] Samarghandi, M.R., Nemattollahi, D., Asgari, G., Shokoohi, R., Ansari, A., Dargahi, A. (2018). Electrochemical Process for 2,4-D Herbicide Removal from Aqueous Solutions Using Stainless Steel 316 and Graphite Anodes: Optimization Using Response Surface Methodology. *Separation Science and Technology (Philadelphia)*, 54(4), 478–493. DOI: 10.1080/01496395.2018.1512618.

[46] Zou, J., Peng, X., Li, M., Xiong, Y., Wang, B., Dong, F., Wang, B. (2017). Electrochemical Oxidation of COD from Real Textile Wastewaters: Kinetic Study and Energy Consumption. *Chemosphere*, 171, 332–338. DOI: 10.1016/j.chemosphere.2016.12.065.

[47] Kapałka, A., Joss, L., Anglada, Á., Comninellis, C., Udert, K.M. (2010). Direct and Mediated Electrochemical Oxidation of Ammonia on Boron-Doped Diamond Electrode. *Electrochemistry Communications*, 12(12), 1714–1717. DOI: 10.1016/j.elecom.2010.10.004.

[48] Wang, Y., Guo, X., Li, J., Yang, Y., Lei, Z., Zhang, Z. (2012). Efficient Electrochemical Removal of Ammonia with Various Cathodes and Ti/RuO-Pt Anode. *Open Journal of Applied Sciences*, 02(04), 241–247. DOI: 10.4236/ojapps.2012.24036.

[49] Yao, J., Mei, Y., Xia, G., Lu, Y., Xu, D., Sun, N., Wang, J., Chen, J. (2019). Process optimization of Electrochemical Oxidation of Ammonia to Nitrogen for Actual Dyeing Wastewater Treatment. *International Journal of Environmental Research and Public Health*, 16(16) DOI: 10.3390/ijerph16162931.

[50] Yuan, F., Dai, J.G., Liang, Z.H., Fan, H.B., Lv, S.H. (2013). Study on the Conversion of Ammonia by Electrochemical Oxidation. *Advanced Materials Research*, 807–809, 1355–1361. DOI: 10.4028/www.scientific.net/AMR.807-809.1355.

[51] Mandor, H., El-Ashtoukhy, E.S.Z., Abdelwahab, O., Amin, N.K., Kamel, D.A. (2022). A Flow-Circulation Reactor for Simultaneous Photocatalytic Degradation of Ammonia and Phenol Using N-Doped ZnO Beads. *Alexandria Engineering Journal*, 61(5), 3385–3401. DOI: 10.1016/j.aej.2021.08.052.